https://doi.org/10.5194/egusphere-2026-4493
Preprint. Discussion started: 17 August 2026

Environmental impacts of polarity-resolved water-soluble organic matter from animal dung burning on the Qinghai-Tibet Plateau

Shasha Huang[1], Zhenxing Shen[1*], Cailan Li[1], He Shen[1], Yaling Zeng[2], Liu Yang[1], Jian Sun[1], Hongmei Xu[1]

[1] *Department of Environmental Sciences and Engineering, Xi'an Jiaotong University, Xi'an, 710049, China*

[2] *School of Environmental Science and Engineering, Southern University of Science and Technology, 518055, Shenzhen, China*

*Author to *whom correspondence should be addressed.*

E-mail: zxshen@mail.xjtu.edu.cn (Zhenxing Shen)

https://doi.org/10.5194/egusphere-2026-4493
Preprint. Discussion started: 17 August 2026

Abstract

Animal dung was widely used for rural heating and cooking on the Qinghai-Tibet Plateau (QTP), its contributions to climate-relevant and health-related aerosol properties remain poorly understood. In this study, water-soluble organic matter (WSOM), which separated into neutral humic-like substances (HULIS-n), acidic humic-like substances (HULIS-a), and highly polar WSOM (HP-WSOM), in $PM_{2.5}$ from yak and sheep dung on the QTP were conducted to evaluate their radiative forcing and oxidative potential (OP). It showed that HULIS-a and HULIS-n exhibited the highest emission factors under heating (0.80±0.46 g/kg) and cooking (0.35±0.36 g/kg) scenarios, respectively. HULIS-n exhibited the strongest light absorption compared to the highest OP for HP-WSOM. Total WSOM-C emissions from animal dung combustion on the QTP were 7.5 Gg and 2.0 Gg for heating and non-heating season, with sheep dung for heating contributing the largest (40.6%). Spatial distributions of radiative forcing and OP were highly correlated with the intensity of sheep dung. The estimated radiative forcing of WSOM corresponded to 10.9–34.7% of black carbon, suggesting that WSOM may be an important contributor to regional atmospheric warming and cryosphere change on the QTP. Scenario analysis showed that replacing 50% of sheep dung combustion with yak dung could reduce regional radiative forcing and OP by 2.4×10^4 MW/km^2 and 948.8 $(AU\ s^{-1}g^{-1})/km^2$. These findings highlight the importance of animal dung combustion to light-absorbing and redox-active organic aerosols on the QTP and provide scientific support for cleaner household energy strategies and fuel-use optimization in the region.

Key words: Qinghai-Tibet plateau, Animal dung, Water-soluble organic matter, Radiative forcing, Health effect

1. Introduction

https://doi.org/10.5194/egusphere-2026-4493
Preprint. Discussion started: 17 August 2026

The Qinghai-Tibet Plateau (QTP) is one of the most climatically sensitive regions in the world and plays a critical role in regulating the Asian water cycle and regional climate. Covering approximately 26.0% of China's total land area, the QTP is characterized by high elevations, low atmospheric pressure, and a cold climate (Chen et al., 2015). In the agricultural and pastoral areas of the QTP, animal dung, primarily from yak dung and sheep, remains an important household fuel for cooking and heating because of its widespread availability and low cost (Chen et al., 2018; Hu et al., 2016). Due to limited access to modern energy sources and the long heating season, large quantities of animal dung are burned annually, making residential combustion a major source of atmospheric pollutants on the QTP (Sun et al., 2021; Zhang et al., 2022a).

The unique high-altitude environment of the QTP can substantially influence combustion processes. Reduced oxygen availability often leads to incomplete combustion, resulting in elevated emissions of particulate matter (PM), black carbon (BC), brown carbon (BrC), polycyclic aromatic hydrocarbons (PAHs), and other hazardous pollutants (Guan et al., 2017; Sun et al., 2021). These emissions can affect regional air quality, human health, and climate. In particular, light-absorbing carbonaceous aerosols deposited on snow and glacier surfaces can reduce albedo and accelerate glacier melting, thereby influencing hydrological processes and regional climate change across the plateau.

Among carbonaceous aerosol components, water-soluble organic matter (WSOM) represents an important fraction of BrC. WSOM contains numerous chromophoric compounds capable of absorbing solar radiation and contributing to atmospheric warming. Humic-like substances (HULIS), which constitute a major fraction of WSOM, have been widely identified in emissions from biomass burning, coal combustion, and ambient aerosols (Cao et al., 2021; Fan et al., 2016; Huo et al., 2021; Zhang et al., 2021). Previous studies have shown that HULIS can account for a substantial fraction of WSOM light absorption and contribute significantly to the radiative effects of organic aerosols (Chung et al., 2012; Mo et al., 2018). In addition to their climatic impacts, HULIS and other WSOM components can participate in redox reactions and generate reactive oxygen species (ROS), thereby contributing to the oxidative potential (OP) of atmospheric particles (Campbell et al., 2021; Charrier and Anastasio, 2012a; Xu et al., 2020). Elevated OP has been linked to oxidative stress and adverse respiratory and cardiovascular outcomes associated with particulate matter exposure.

Recent studies have demonstrated that WSOM is chemically heterogeneous and can be separated into fractions with distinct physicochemical properties. Mukherjee et al. (2020) classified WSOM into neutral humic-like substances (HULIS-n), acidic humic-like substances (HULIS-a), and highly polar WSOM (HP-WSOM). These fractions differ substantially in their molecular composition, optical characteristics, hygroscopicity, and redox activity (Chen et al., 2016a, b; Zhou et al., 2021). For example, HULIS-n has been reported to dominate the light absorption of WSOM, whereas highly polar fractions often contain oxygenated compounds that may contribute disproportionately to oxidative activity. However, most previous studies have focused on urban aerosols or emissions from conventional biomass and coal combustion, while information on polarity-resolved WSOM emitted from animal dung combustion remains very limited. Although several studies have characterized emissions of PM, PAHs, volatile organic compounds, and carbonaceous aerosols from yak and sheep dung combustion on the QTP (Hu et al., 2016; Sun et al., 2021; Zhang et al., 2022a), the optical and oxidative properties of different WSOM fractions have not been systematically investigated. Furthermore, the regional implications of these emissions for climate-relevant radiative forcing and health-related OP remain poorly quantified. Given the extensive use of animal dung fuels and the environmental sensitivity of the QTP, a comprehensive assessment of polarity-resolved WSOM emissions and their potential impacts is urgently needed.

In this study, field combustion experiments were conducted to characterize HULIS-n, HULIS-a, and HP-WSOM emitted from yak and sheep dung burning under representative heating and cooking conditions on the QTP. The optical properties,

https://doi.org/10.5194/egusphere-2026-4493
Preprint. Discussion started: 17 August 2026

chemical functional groups, and OP of these WSOM fractions were investigated. Based on measured emission factors and county-level activity data, regional inventories of WSOM emissions, radiative forcing potential, and OP were developed for the QTP. The specific objectives of this study were to: (1) characterize the emission profiles and physicochemical properties of polarity-resolved WSOM from animal dung combustion; (2) quantify the spatial and temporal distributions of WSOM emissions, radiative forcing potential, and OP across the QTP; and (3) evaluate the potential environmental and health implications of animal dung combustion and explore possible mitigation strategies.

2. Experiments and Methods

2.1. Sample collection

The field experiment was conducted in herder's home in Gangcha County, a major breeding area for yaks and Tibetan sheep. The heating season lasted from September to May of the following year. The yak and sheep dung used in this study were air-dried, and the bituminous coal was purchased from the local market (H: heating, C: cooking, YD: yak dung, SD: sheep dung). The stoves used in this study had both cooking and heating functions and were controlled by an intake valve. Detailed elemental composition of the three fuels and the stove settings for heating and cooking scenarios can be found in the study by Sun et al. (2021). $PM_{2.5}$ samples were collected with a quartz fiber filter membrane (Whatman Inc, Clifton, NJ, USA) at a flow rate of 5 L min^{-1} using a Mini-sampler (Air metrics, Eugene, OR, USA). Following collection, $PM_{2.5}$ samples were stored at -4°C for subsequent experiments and analysis. The separation and extraction methods for the three types of WSOM are described in detail in Text S1.

2.2. Determination of optical properties

A USB2000+UV-vis-es spectrometer equipped with a 100 cm long liquid waveguide capillary cell 3100 (LWCC-3100, World Precision Instruments, Sarasota, FL, USA) was used to determine the light absorption of the three types of WSOM in the UV-visible range (200-800 nm). The detailed calculation process of the mass

https://doi.org/10.5194/egusphere-2026-4493
Preprint. Discussion started: 17 August 2026

absorption efficiency (MAE), $b_{abs-365}$, and simple forcing efficiency (SFE) for HULIS-n, HULIS-a, and HP-WSOM is documented in detail in Text S2.

2.3. Determination of chemical composition and OP

The chemical functional groups of WSOM were analyzed by Fourier transform infrared spectroscopy (FT-IR) equipped with an attenuated total reflection module (Perkin Elmer, model Spectrum one) to determine the molecular structure characteristics of the three types of WSOM. HULIS-n, HULIS-a, and HP-WSOM were loaded on KBr pellets and fully ground to obtain the mean value of 64 scans in the spectrum range of 300-4000 cm^{-1} (resolution 4 cm^{-1}). The detailed operation procedure was found in the previous study (Huang et al., 2022; Zhang et al., 2022c).

In this study, the OP of the three types of WSOM was determined using a dichlorofluorescein diacetate (DCFH-DA) probe (Sigma-Aldrich, Saint Louis, MO, USA). A certain volume of WSOM was added to a 96-well plate for both the samples and controls, along with Hanks balanced salt buffer and DCFH, and incubated for 10 min at room temperature under dark conditions. A microplate reader (Gene Company Limited, Synergy LX) was used to characterize the OP of the three types of WSOM by measuring the fluorescence intensity for 0 min and 30 min at 485 nm and 538 nm excitation emission wavelengths (Zhang et al., 2022b).

2.4. Calculation of emission inventories

The EF used in this study is based on our field measurements and estimated for HULIS-n, HULIS-a, HP-WSOM content, $SFE_{200-700}$, and OP. The emissions, health effects and environmental effects of the three types of WSOM produced by animal dung combustion at county level were calculated by using the amount of animal dung combustion and the corresponding EF.

The calculation formula for the heating season is as follows:

$$E_{H,i,l,j} = (1 - r) \times \varphi \times A_{i,k} \times EF_{c,k,j} + (1 - r) \times (1 - \varphi) \times A_{i,k} \times EF_{h,k,j} \quad (1)$$

The calculation formula for the non-heating season is as follows:

$$E_{C,i,k,j} = r \times A_{i,k} \times EF_{c,k,j} \quad (2)$$

where E is the pollutant emission, ton (t) t; r is the share of yak/sheep dung

https://doi.org/10.5194/egusphere-2026-4493
Preprint. Discussion started: 17 August 2026

combustion consumption in the non-heating season to the total annual consumption; A is the total yak/sheep dung consumption, Gigagram (Gg); EF is the EF of pollutant content, $SFE_{200\text{-}700}$, and OP; φ is the proportion of dung consumed for cooking in the heating season; C denotes cooking activity; H is heating activity; C denotes non-heating season; H denotes heating season; I denotes county. K represents animal type (yak or sheep); j represents pollutant type. r and φ values were determined based on studies by (Hu et al., 2016) and were set at 31.0% and 51.2%, respectively.

A Monte Carlo simulation was used to analyze the uncertainty in the emission inventory. Activity data and EFs were the determinants of uncertainty and they are assumed to be normally distributed. The activity data and the input parameters of the EFs with their corresponding measurements were entered into the Monte Carlo framework using the Crystal Ball software. A total of 20,000 runs were performed for each data set to ensure a valid simulation for analyzing uncertainty. In this study, uncertainty refers to the 95% confidence interval of the mean estimate.

3. Results and Discussion

3.1. General characteristics of WSOM emissions from animal dung combustion

During the combustion of yak and sheep dung, HULIS-a-C and HULIS-n-C exhibited the highest EFs, averaging 0.80±0.46 g/kg and 0.35±0.36 g/kg from heating and cooking scenarios, respectively, whereas HP-WSOM-C showed the lowest EF (Figure 1a). Light absorption analysis revealed that HULIS-n possessed the strongest light absorption capacity, with the highest MAE_{365} (8.01±6.66 m^2/g) and EF of $b_{abs\text{-}365}$ (219.39±212.81 m^2/g) for both heating and cooking (Figure 1b), while HULIS-a and HP-WSOM had the lowest MAE_{365} and EF of $b_{abs\text{-}365}$, respectively. In terms of potential health risks, HP-WSOM displayed the highest OP among all combustion scenarios except C-SD. Its OP was 1.3~3.0 and 4.0~11.4 times higher than those of HULIS-n and HULIS-a, respectively. This trend contrasts sharply with their light absorption characteristics, suggesting that differences in functional group composition govern their optical and oxidative properties.

https://doi.org/10.5194/egusphere-2026-4493
Preprint. Discussion started: 17 August 2026

Analysis of functional groups (Figure S1) showed that HULIS-n contains higher abundances of organic nitrates (1634 cm^{-1} or 833 cm^{-1}), aromatic hydrocarbons and phenolic hydroxyl compounds (1260 cm^{-1}). Organic nitrates and aromatic compounds are known chromophores in organic aerosols and contribute strongly to light absorption. In particular, nitrogen-containing aromatic compounds have been reported to account for 55% of WSOM absorbance (Desyaterik et al., 2013). The organic nitrate and aromatic structures render HULIS-n the most light-absorbing substance in WSOM. HP-WSOM exhibited the strongest polarity and was enriched in carboxylic acids, polysaccharides, and other hydrophilic compounds (1220 cm^{-1} and 1053 cm^{-1}). The weak light absorption of carboxylic acids, coupled with the lowest EF of HP-WSOM, resulted in its low light absorption. Nevertheless, HP-WSOM contains substantial amounts of redox-active aromatic compounds, including quinones (Figure S1c, 1716 cm^{-1}) and transition metals. Organic compounds can generate oxidative stress through redox of quinone-based radicals, and metals can directly support electron transfer to generate OP while reducing antioxidant levels. Quinones can induce oxidative stress through redox cycling and formation of semiquinone radicals, while transition metals facilitate electron-transfer reactions that enhance reactive oxygen species (ROS) generation and deplete antioxidants (Charrier and Anastasio, 2012b; Gonzalez et al., 2017; Guo et al., 2020; Lin and Yu, 2019a, b; Lin and Yu, 2020; Win et al., 2018). These components likely account for the elevated OP of HP-WSOM despite its weak optical absorption. In contrast, HULIS-a was characterized by a higher abundance of carboxyl-containing compounds and a lower proportion of strongly light-absorbing components, such as aromatic and nitrate-containing species. Consequently, HULIS-a exhibited both lower light absorption and lower oxidative potential than the other WSOM fractions.

https://doi.org/10.5194/egusphere-2026-4493
Preprint. Discussion started: 17 August 2026

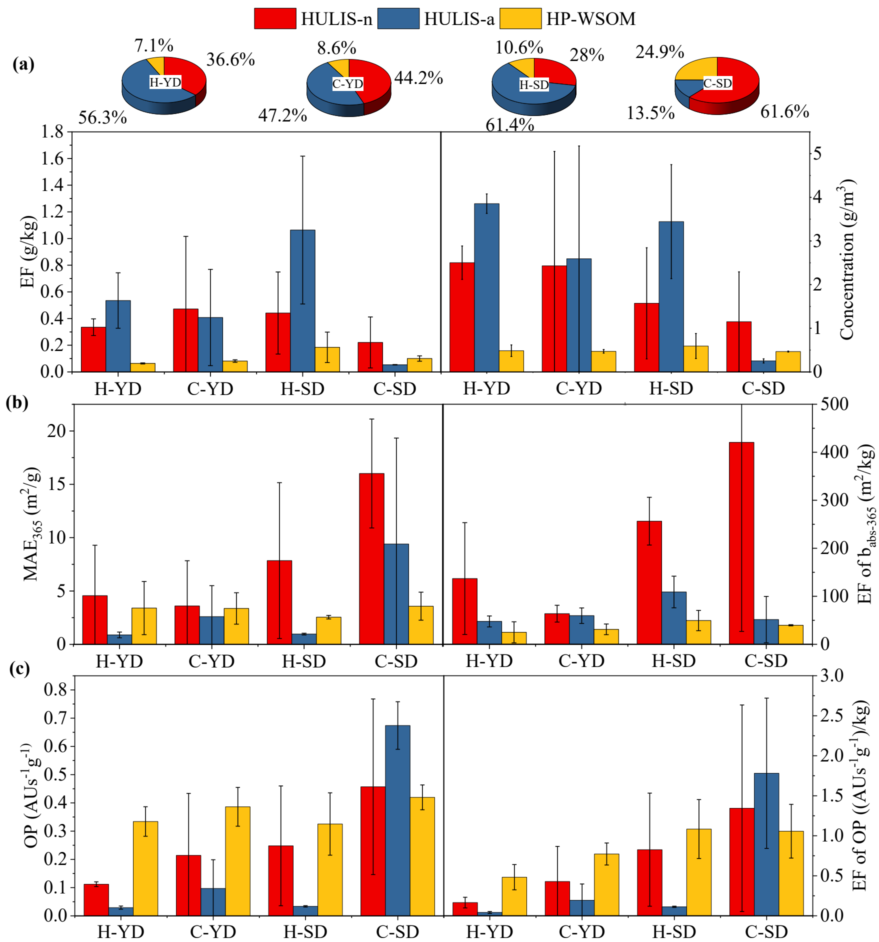

Figure 1. Emission factors (EFs) and concentrations (a), MAE_{365} and EFs of $b_{abs\text{-}365}$ (b), and OP and EFs of OP (c) for HULIS-n, HULIS-a, and HP-WSOM emitted from sheep and yak dung combustion under heating and cooking scenarios.

3.2. Emission inventory and spatial distribution of HULIS

The total emissions of WSOM from yak and sheep dung combustion on the QTP were estimated (Figure 2a). Total WSOM-C emissions during the heating and non-heating season were 7.5 and 2.0 Gg, respectively. During the heating season, annual emissions of HULIS-n-C, HULIS-a-C, and HP-WSOM-C reached 2.6, 3.9, and 0.9 Gg, respectively, representing increases of 1.5-, 6.1-, and 2.8-fold compared with the non-

https://doi.org/10.5194/egusphere-2026-4493
Preprint. Discussion started: 17 August 2026

heating season. The highest emissions of HULIS-n, HULIS-a, and HP-WSOM were observed in Gonghe county.

Among the four combustion scenarios, yak dung for heating, yak dung for cooking, sheep dung for heating, and sheep dung for cooking contributed 13.7%, 27.9%, 40.6%, and 17.8% of total WSOM emissions, respectively. Sheep dung for heating was the primary source of WSOM-C, accounting for 26.7%, 53.4%, and 35.4% of the total emission of HULIS-n-C, HULIS-a-C, and HP-WSOM-C, respectively. Zhang et al. (2022) and He et al. (2024) showed that sheep dung for heating was the largest source of PAHs and intermediate volatile organic compounds (IVOCs) from animal dung combustion on the QTP. These findings highlight the critical role of sheep dung combustion during the heating season in the emission and formation of air pollutants across the region.

Spatial differences in emissions among counties are more clearly illustrated by WSOM emission densities (Figure 2b). The annual emission density of WSOM-C was 4.8 kg/km^2, with heating season emissions being 3.8 times higher than those during the non-heating season. Among the WSOM fractions, HULIS-a exhibited the highest emission density (2.3 kg/km^2), accounting for 47.8% of the total WSOM-C emissions. During both the heating and non-heating seasons, the highest emission densities of HULIS-n, HULIS-a, and HP-WSOM were observed in Huangyuan and Huangzhong counties. Huangyuan has a well-developed livestock industry with a grassland vegetation coverage of 64.5%. In addition, sheep dung combustion during the heating season accounts for 58.2% of the total animal dung used in Huangyuan. The combination of intensive livestock production and substantial sheep dung use for residential heating results in the highest WSOM-C emission density in Huangyuan.

https://doi.org/10.5194/egusphere-2026-4493
Preprint. Discussion started: 17 August 2026

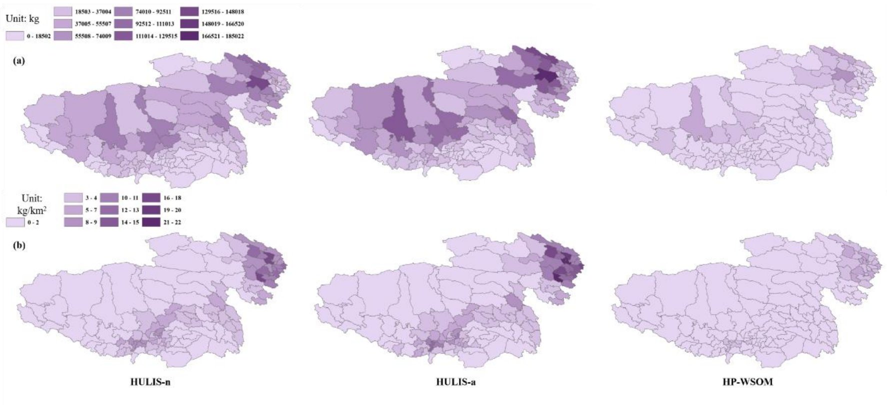

Figure 2. Spatial distributions of the concentrations of HULIS-n, HULIS-a, and HP-WSOM from the combustion of yak dung and sheep dung on the QTP.

3.3 *Spatiotemporal distribution of environmental effects and health impacts*

WSOM emitted from animal dung combustion can contribute to regional radiative forcing through its light-absorbing properties. The highest $SFE_{200-700}$ values for the combustion of yak dung and sheep dung were observed for HP-WSOM and HULIS-n, respectively (Table 1), whereas HULIS-a exhibited the lowest $SFE_{200-700}$ among the four combustion scenarios. The emission inventory shows that the total WSOM-induced radiative forcing during the heating season was 1.4 times that during the non-heating season (Figure S2). HULIS-a and HULIS-n were the largest contributors to radiative forcing during the heating and non-heating season, accounting for 35.1% and 40.0% of total WSOM radiative forcing, respectively. On the QTP, radiative forcing associated with HULIS-n, HULIS-a, and HP-WSOM during the heating season was 1.1, 1.3, and 2.1 times higher, respectively, than during the non-heating season.

Table 1. The SFE of HULIS-n, HULIS-a, and HP-WSOM from the combustion of yak dung and sheep dung for heating and cooking.

SFE (W/g)	Sample	Yak dung-heating	Yak dung-cooking	Sheep dung-heating	Sheep dung-cooking
SFE_{280-}	HULIS-n	21.8 ± 21.5	21.3 ± 23.8	43.3 ± 39.8	83.8 ± 16.6

https://doi.org/10.5194/egusphere-2026-4493
Preprint. Discussion started: 17 August 2026

700	HULIS-a	7.8 ± 1.9	22.4 ± 26.2	9.1 ± 0.6	76.8 ± 7.6
	HP-WSOM	31.3 ± 19.8	30.7 ± 15.1	28.2 ± 7.4	32.7 ± 6.5

Spatially, the radiative forcing per unit area from WSOM was highest in Huangyuan county and lowest in Medog county, reflecting regional differences in livestock density and dung-fuel consumption. Among the four combustion scenarios, yak dung for heating, yak dung for cooking, sheep dung for heating, and sheep dung for cooking contributed 6.3%, 15.2%, 13.7%, and 64.7% to the total WSOM radiative forcing, respectively (Figure 3c1). Radiation forcing from the combustion of yak dung and sheep dung for cooking was 2.4 and 4.7 times higher, respectively, than that for heating. Sheep dung combustion contributes 72.5% and 80.9% to total radiative forcing during the heating and non-heating season, respectively, representing contributions 2.6 and 4.2 times higher than those from yak dung combustion. These results indicate that sheep dung combustion, particularly for cooking, is the dominant source of WSOM-induced radiative forcing on the QTP and therefore poses a greater environmental burden than yak dung combustion.

Earlier studies have demonstrated that both modeled and measured OP of $PM_{2.5}$ are associated with cardiovascular and respiratory health effects (Abrams et al., 2017). Moreover, OP has been shown to correlate more strongly with adverse health effects than $PM_{2.5}$ mass concentration, highlighting its value as an indicator of aerosol toxicity (Janssen et al., 2015). The total OP of WSOM emitted from yak dung and sheep dung combustion during the heating season was 1.7 times higher than that during the non-heating season (Figure S3). HP-WSOM and HULIS-a were the dominant contributors to OP during the heating and non-heating season, accounting for 38.6% and 37.7% of the total WSOM OP, respectively. During the heating season, the OP associated with HULIS-n, HULIS-a, and HP-WSOM was 1.7, 1.2, and 2.2 times higher, respectively, than during the non-heating season.

https://doi.org/10.5194/egusphere-2026-4493
Preprint. Discussion started: 17 August 2026

The spatial distributions of OP for HULIS-n, HULIS-a, and HP-WSOM closely resembled those of WSOM emissions and radiative forcing, with the highest values observed in Huangyuan county and the lowest in Medog county (Figure 3b). However, yak dung for heating, yak dung for cooking, sheep dung for heating, and sheep dung for cooking accounted for 3.4%, 13.6%, 16.4%, and 66.6% of the total WSOM OP, respectively (Figure 3c2). These results clearly indicate that the health impacts associated with WSOM are dominated by sheep dung combustion for cooking. The combustion of sheep dung contributed 82.9% and 83.0% to the total OP during the heating and non-heating season, respectively, which is 4.9 times that of yak dung. The OP from the combustion of sheep dung accounted for 84.9%, 93.3%, and 72.0% of the OP of HULIS-n, HULIS-a, and HP-WSOM, respectively, which is 5.6, 13.9, and 2.6 times higher than that from yak dung combustion. These findings suggest that the environmental and health impacts of WSOM from animal dung combustion exhibit similar spatial and seasonal patterns and are strongly associated with the extent of sheep dung combustion.

Table S1 lists the uncertainty ranges of carbon emission estimates for HULIS-n, HULIS-a, and HP-WSOM, which are -52.9% – 303%, -65.7% – 319%, and -54.7% – 290%, respectively. Among the three fractions, HULIS-a exhibited the highest uncertainty. The activity data used in this inventory were sourced from official governmental statistical yearbooks, which are generally considered reliable and contain relatively small uncertainties for regional emission estimation. Furthermore, the use of localized and detailed activity data allows a more accurate representation of actual fuel-use patterns and livestock distributions, thereby reducing uncertainty in the emission inventory. Consequently, the emission estimates presented in this study are considered reasonably robust and representative of WSOM emissions from animal dung combustion on the QTP.

https://doi.org/10.5194/egusphere-2026-4493
Preprint. Discussion started: 17 August 2026

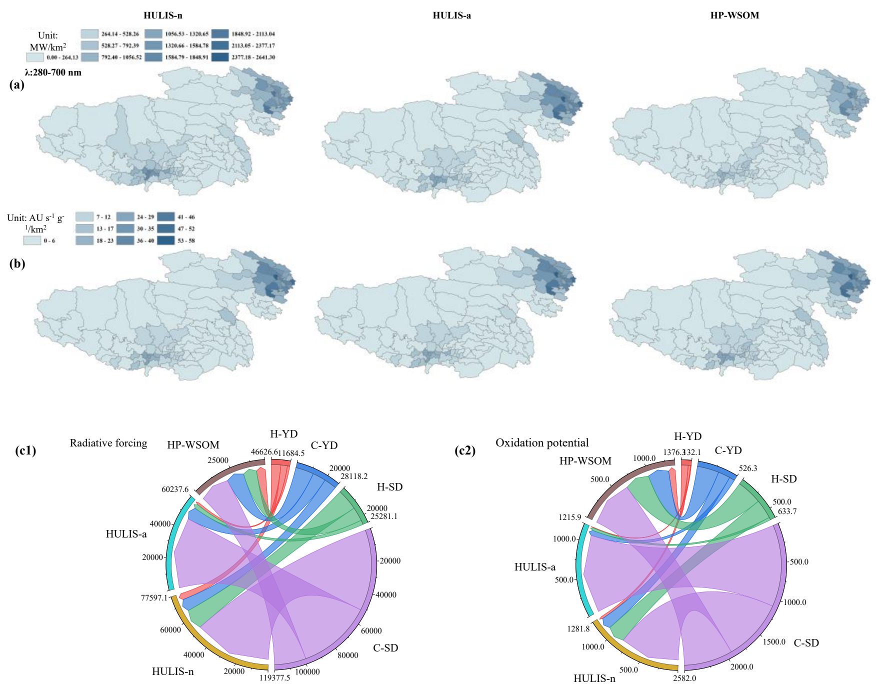

Figure 3. The distribution of radiative forcing and OP of HULIS-n, HULIS-a, and HP-WSOM from the combustion of yak dung and sheep dung on QTP, and the proportion of WSOM contributed by different burning scenarios.

3.4. Implications of Environmental and health effects of WSOM on the QTP

The air supply for heating during the combustion of sheep and yak dung was lower than that for cooking. Correspondingly, the EFs of WSOM-C from sheep and yak dung combustion for heating were 1.2 and 4.5 times higher, respectively, than those from cooking. This indicates that oxygen-deficient combustion enhanced WSOM emissions. The MAE_{365} and EF of $b_{abs\text{-}365}$ from animal dung and bituminous coal combustion on the QTP are 2.1–14.3 and 27.3–169.7 times higher, respectively, than those from biomass and bituminous coal combustion on the Fen-Wei Plain (Table S2). The QTP is characterized by thin air, low air pressure, and reduced oxygen availability (Cui et al., 2023; Tian et al., 2023). Under such oxygen-limited conditions, generation of free radicals is suppressed, hindering oxidation reactions during combustion (Jiang et al.,

https://doi.org/10.5194/egusphere-2026-4493
Preprint. Discussion started: 17 August 2026

2023). Therefore, oxygen-deficient combustion is a key factor controlling WSOM emissions and associated environmental impacts on the QTP.

More importantly, the $SFE_{200\text{-}700}$ of atmospheric BC on the QTP has been reported to be 558 W/g (Wang et al., 2019). In comparison, the $SFE_{200\text{-}700}$ of WSOM emitted from yak and sheep dung combustion in the present study ranged from 61.0 to 193.4 W/g, corresponding to 10.9–34.7% of the BC radiative forcing (Table 1). Light-absorbing carbonaceous aerosols, such as BC, can significantly reduce snow albedo even at concentrations as low as 10 ng/g, thereby generating positive radiative forcing at the snow and ice surface and increase near-surface air temperature (Flanner et al., 2007; 2009). Glacier albedo has also been shown to be highly sensitive to HULIS-like light-absorbing substances (Wu et al., 2016). Consequently, emissions from oxygen-deficient combustion of yak and sheep dung may play an important role in influencing the cryosphere and regional hydrological cycle of the QTP.

According to the China Health and Aging Tracking Survey, exposure to air pollution from household solid fuel combustion increases the risk of developing chronic obstructive disease, heart disease, and stroke (Liu et al., 2023; Qiu et al., 2019; Wang et al., 2020). The OP of WSOM emitted from the combustion of yak dung, sheep dung, and bituminous coal on the OTP is 4.9–43.8 times higher than that of WSOM from the combustion of biomass and bituminous coal on the Fen-Wei Plain (Table S2). These results indicate that WSOM generated under oxygen-deficient combustion conditions may pose substantially greater health risks. Considering the long-term environmental and health consequences, it is essential to develop sustainable animal-dung management strategies and promote cleaner energy alternatives in the region.

The QTP region possesses abundant solar and wind energy resources (Fang et al., 2013), which offer considerable potential for reducing both air pollutants emissions and carbon emissions (Wang et al., 2023). In addition, Cai et al. (2014) reported that sheep dung emits less N_2O and CO_2 during composting than yak dung, and that emissions from both dung types are lower than the default values recommended by the IPCC.

https://doi.org/10.5194/egusphere-2026-4493
Preprint. Discussion started: 17 August 2026

However, the results presented in Sections 3.2 and 3.3 revealed that sheep dung combustion produces stronger pollutant emission and environmental impacts than yak dung combustion. Therefore, a practical mitigation strategy may involve composting a larger fraction of sheep dung for agricultural application while preferentially using yak dung as a household fuel for cooking and heating. Based on our calculations, replacing 50% of sheep dung combustion with yak dung combustion could reduce radiative forcing and OP densities across the QTP by 2.4×10^4 MW/km^2 and 948.8 (AU s^{-1}g^{-1})/km^2, respectively. These findings demonstrate that optimizing household fuel-use patterns could effectively mitigate the environmental and health impacts associated with animal dung combustion on the QTP.

To further investigate regional disparities, Lorenz curves and Gini coefficients were used to examine the relationship between county-level per capita GDP and WSOM emissions (Figure 4). The Lorenz curves for HULIS-n, HULIS-a, and HP-WSOM all deviate substantially from the line of perfect equality, yielding Gini coefficients of 0.603, 0.604, and 0.615, respectively. These similar Gini coefficients indicate that the three WSOM fractions exhibit comparable relationships with regional economic development. Huangyuan county ranks 90th in per capita GDP, yet exhibited relatively high pollutant concentration, radiative forcing density, and OP densities. In contrast, Mangya county, which had the second-highest per capita GDP among all the districts and counties in this study area, experienced comparatively low WSOM-related environmental and health impacts. These patterns suggest that pollution burdens tend to be greater in economically less-developed regions. Therefore, priority should be given to implementing animal dung replacement and clean-energy transition programs in areas such as Huangyuan, Minhe, and Tongde, where such measures could substantially reduce the environmental and health impacts associated with animal dung combustion across the QTP.

https://doi.org/10.5194/egusphere-2026-4493
Preprint. Discussion started: 17 August 2026

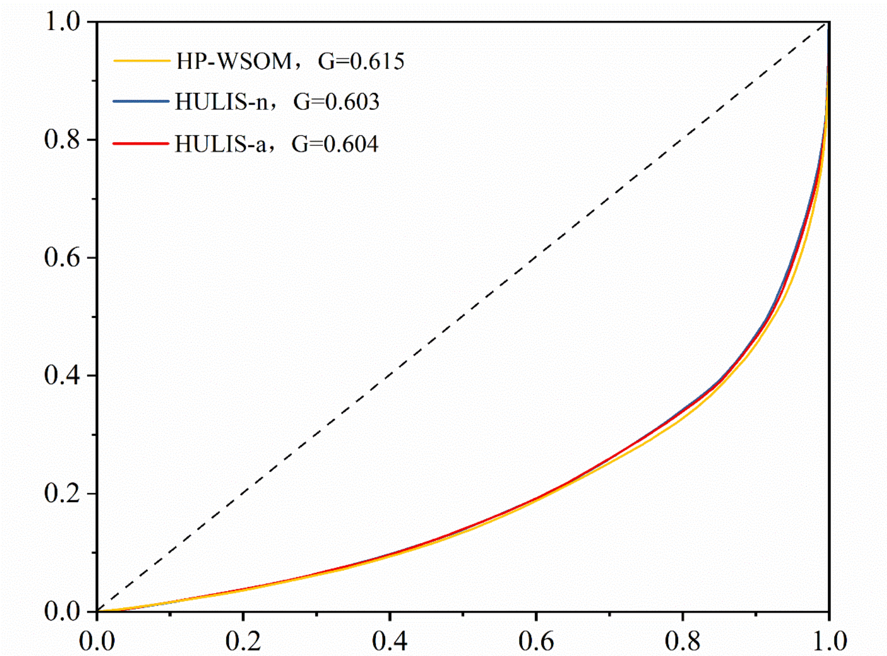

Figure 4. Lorentz curves between HULIS-n, HULIS-a, HP-WSOM and GDP per capita.

4. Conclusions

This study quantified the emissions, radiative effects, and health implications of WSOM emitted from the combustion of yak dung and sheep dung for heating and cooking on the QTP. Nitrogen-containing aromatic compounds were identified as the primary contributor to the light absorption of HULIS-n, while quinone aromatic substances were largely responsible for the elevated OP of HP-WSOM. Among the investigated sources, sheep dung for heating produced the highest WSOM emissions, while sheep dung for cooking generated the greatest combined climate and health impacts.

WSOM emissions, radiative forcing, and OP were substantially higher during the heating season than non-heating season, highlighting the importance of wintertime household energy use. The oxygen-deficient combustion conditions prevalent on the QTP further enhanced WSOM emissions, exacerbating both climate and health risks. Notably, WSOM from the combustion of yak and sheep dung accounted for 10.9–34.7%

https://doi.org/10.5194/egusphere-2026-4493
Preprint. Discussion started: 17 August 2026

of the radiative forcing of BC on the QTP, demonstrating that WSOM is a previously underappreciated driver of regional warming and may play a significant role in accelerating glacier retreat on the QTP.

Scenario analysis showed that replacing 50% of sheep dung with yak dung as a household fuel could reduce radiative forcing and OP by 2.4×10^4 MW/km^2 and 948.8 (AU s^{-1}g^{-1})/km^2, respectively, indicating substantial co-benefits for climate mitigation and public health. Given the relatively low implementation costs, such fuel-substitution strategies should be prioritized in economically underdeveloped areas, including Huangyuan County. In summary, the inventories of WSOM content, radiative forcing, and OP from yak and sheep dung combustion generated in this study provided the much-needed data for accurately assessing the impacts of household energy use on climate, glaciers, and residents' health. The identified mitigation strategies provided a practical pathway for reducing both environmental and health burdens in high-altitude communities.

Data availability

The key datasets are publicly available on the Zenodo data repository platform: https://doi.org/10.5281/zenodo.21306255, 2026 (Huang, 2026).

Author contribution

ZS: Conceptualization. SH, CL, and HS: Data curation. ZS and HX: Funding acquisition. SH and YZ: Methodology. ZS: Resources. SH: Writing - original draft. SH, ZS, LY, HX, JS: Writing - review & editing.

https://doi.org/10.5194/egusphere-2026-4493
Preprint. Discussion started: 17 August 2026

Competing interests

The authors declare that they have no conflict of interest.

Acknowledgements

This research was supported by the National Natural Science Foundation of China (42477238; 41877383), and a grant from Shaanxi Key Laboratory of Environmental Monitoring and Forewarning of Trace Pollutions, Shaanxi Environmental Monitoring Center station (SHJKFJJ202308).

Reference

Abrams, J.Y., Weber, R.J., Klein, M., Sarnat, S.E., Chang, H.H., Strickland, M.J., Verma, V., Fang, T., Bates, J.T., Mulholland, J.A., Russell, A.G., Tolbert, P.E.: Associations between Ambient Fine Particulate Oxidative Potential and Cardiorespiratory Emergency Department Visits. Environmental Health Perspectives, 125, https://doi.org/10.1289/EHP1545, 2017.

Afsana, S., Zhou, R.C., Miyazaki, Y., Tachibana, E., Deshmukh, D.K., Kawamura, K., Mochida, M.: Abundance, chemical structure, and light absorption properties of humic-like substances (HULIS) and other organic fractions of forest aerosols in Hokkaido. Scientific Reports, 12, https://doi.org/10.1038/s41598-023-40936-6, 2022.

Bai, L., Lu, X., Yin, S., Zhang, H., Ma, S., Wang, C., Li, Y., Zhang, R.: A recent emission inventory of multiple air pollutant, $PM_{2.5}$ chemical species and its spatial-temporal characteristics in central China. Journal Of Cleaner Production 269. https://doi.org/10.1016/j.jclepro.2020.122114, 2020.

Bellouin, N., Quaas, J., Morcrette, J.J., Boucher, O.: Estimates of aerosol radiative forcing from the MACC re-analysis. Atmos. Chem. Phys. 13, 2045-2062. https://doi.org/10.5194/acp-13-2045-2013, 2013.

Bond, T.C., Bergstrom, R.W.: Light absorption by carbonaceous particles: An investigative review. Aerosol Science And Technology, 40, 27-67, https://doi.org/10.1080/02786820500421521, 2006.

Campbell, S.J., Wolfer, K., Utinger, B., Westwood, J., Kalberer, M.: Atmospheric conditions and

https://doi.org/10.5194/egusphere-2026-4493
Preprint. Discussion started: 17 August 2026

composition that influence $PM_{2.5}$ oxidative potential in Beijing, China. Atmos. Chem. Phys, 21, 5549-5573, https://doi.org/10.5194/acp-21-5549-2021, 2021.

Cao, T., Li, M., Zou, C., Fan, X., Peng, P.A.: Chemical composition, optical properties, and oxidative potential of water- and methanol-soluble organic compounds emitted from the combustion of biomass materials and coal. Atmos. Chem. Phys, 21, 13187-13205, https://doi.org/10.5194/acp-21-13187-2021, 2021.

Charrier, J.G., Anastasio, C.: On dithiothreitol (DTT) as a measure of oxidative potential for ambient particles: evidence for the importance of soluble transition metals. Atmos Chem Phys, 12, 11317-11350, https://doi.org/10.5194/acp-12-9321-2012, 2012a.

Charrier, J.G., Anastasio, C.: On dithiothreitol (DTT) as a measure of oxidative potential for ambient particles: evidence for the importance of soluble transition metals. Atmos. Chem. Phys, 12, 9321-9333, https://doi.org/10.5194/acp-12-9321-2012, 2012b.

Chen, G., Gao, K., Yan, B., Dan, Z., Zhou, W., Cheng, Z.: Estimation and emissions from crop straw and animal dung in Tibet. Sci. Total Environ, 631-632, 1038-1045, https://doi.org/10.1016/j.scitotenv.2018.03.029, 2018.

Chen, J., Shi, W., Cao, J.: Effects of Grazing on Ecosystem CO_2 Exchange in a Meadow Grassland on the Tibetan Plateau During the Growing Season. Environmental Management, 55, 347-359, https://doi.org/10.1007/s00267-014-0390-z, 2015.

Chen, Q., Ikemori, F., Higo, H., Asakawa, D., Mochida, M.: Chemical Structural Characteristics of HULIS and Other Fractionated Organic Matter in Urban Aerosols: Results from Mass Spectral and FT-IR Analysis. Environmental Science & Technology, 50, 1721-1730, https://doi.org/10.1021/acs.est.5b05277, 2016a.

Chen, Q., Ikemori, F., Mochida, M.: Light Absorption and Excitation-Emission Fluorescence of Urban Organic Aerosol Components and Their Relationship to Chemical Structure. Environmental Science & Technology, 50, 10859-10868, https://doi.org/10.1021/acs.est.6b02541, 2016b.

Choudhary, V., Rajput, P., Gupta, T.: Absorption properties and forcing efficiency of light-absorbing water-soluble organic aerosols: Seasonal and spatial variability. Environ. Pollut, 272, https://doi.org/10.1016/j.envpol.2020.115932, 2021.

https://doi.org/10.5194/egusphere-2026-4493
Preprint. Discussion started: 17 August 2026

Chung, C.E., Ramanathan, V., Decremer, D.: Observationally constrained estimates of carbonaceous aerosol radiative forcing. Proc. Natl. Acad. Sci. U. S. A, 109, 11624-11629, https://doi.org/10.1073/pnas.1203707109, 2012.

Cui, L.L., Gao, Y.N., Chen, Y.B., Li, R., Bing, H.J., Wu, Y.H., Wang, G.H.: Chemical characteristics and source apportionment of biogenic primary and secondary organic aerosols in an alpine ecosystem of Tibetan Plateau. J. Geophys. Res.-Atmos, 128, https://doi.org/10.1029/2022JD037897, 2023.

Desyaterik, Y., Sun, Y., Shen, X.H., Lee, T.Y., Wang, X.F., Wang, T., Collett, J.L.: Speciation of "brown" carbon in cloud water impacted by agricultural biomass burning in eastern China. J. Geophys. Res.-Atmos, 118, 7389-7399, https://doi.org/10.1002/jgrd.50561, 2013.

Dong, X.Y., Zhu, Q.Z., Fu, J.S., Huang, K., Tan, J.N., Tipton, M.: Evaluating Recent Updated Black Carbon Emissions and Revisiting the Direct Radiative Forcing in Arctic. Geophysical Research Letters, 46, 3560-3570, https://doi.org/10.1029/2018GL081242, 2019.

Dou, J., Lin, P., Kuang, B.Y., Yu, J.Z.: Reactive Oxygen Species Production Mediated by Humic-like Substances in Atmospheric Aerosols: Enhancement Effects by Pyridine, Imidazole, and Their Derivatives. Environ Sci Technol, 49, 6457-6465, https://doi.org/10.1021/es5059378, 2015.

Fan, X., Wei, S., Zhu, M., Song, J., Peng, P., apos, an.: Comprehensive characterization of humic-like substances in smoke $PM_{2.5}$ emitted from the combustion of biomass materials and fossil fuels. Atmos. Chem. Phys, 16, 13321-13340, https://doi.org/10.5194/acp-16-13321-2016, 2016.

Fang, Y.P., Wei, Y.Q.: Climate change adaptation on the Qinghai-Tibetan Plateau: The importance of solar energy utilization for rural household. Renewable & Sustainable Energy Reviews, 18, 508-518, https://doi.org/10.1016/j.rser.2012.10.037, 2013.

Flanner, M.G., Zender, C.S., Hess, P.G., Mahowald, N.M., Painter, T.H., Ramanathan, V., Rasch, P.J.: Springtime warming and reduced snow cover from carbonaceous particles. Atmos. Chem. Phys, 9, 2481-2497, https://doi.org/10.5194/acp-9-2481-2009, 2009.

Flanner, M.G., Zender, C.S., Randerson, J.T., Rasch, P.J.: Present-day climate forcing and response from black carbon in snow. J. Geophys. Res.-Atmos, 112, https://doi.org/10.1029/2006JD008003, 2007.

Frka, S., Sala, M., Brodnik, H., Stefane, B., Kroflic, A., Grgic, I.: Seasonal variability of

https://doi.org/10.5194/egusphere-2026-4493
Preprint. Discussion started: 17 August 2026

nitroaromatic compounds in ambient aerosols: Mass size distribution, possible sources and contribution to water-soluble brown carbon light absorption. Chemosphere, 299, 134381, https://doi.org/10.1016/j.chemosphere.2022.134381, 2022.

Fu, T.M., Cao, J.J., Zhang, X.Y., Lee, S.C., Zhang, Q., Han, Y.M., Qu, W.J., Han, Z., Zhang, R., Wang, Y.X., Chen, D., Henze, D.K.: Carbonaceous aerosols in China: top-down constraints on primary sources and estimation of secondary contribution. Atmos. Chem. Phys, 12, 2725-2746, https://doi.org/10.5194/acp-12-2725-2012, 2012.

Gonzalez, D.H., Cala, C.K., Peng, Q., Paulson, S.E.: HULIS Enhancement of Hydroxyl Radical Formation from Fe(II): Kinetics of Fulvic Acid-Fe(II) Complexes in the Presence of Lung Antioxidants. Environmental Science and Technology, 51, 7676, https://doi.org/10.1021/acs.est.7b01299, 2017.

Guan, Y., Chen, G., Cheng, Z., Yan, B., Hou, L.a.: Air pollutant emissions from straw open burning: A case study in Tianjin. Atmos. Environ, 171, 155-164, https://doi.org/10.1016/j.atmosenv.2017.10.020, 2017.

Guo, H., Fu, H., Jin, L., Huang, S., Li, X.: Quantification of synergistic, additive and antagonistic effects of aerosol components on total oxidative potential. Chemosphere, 252, 126573, https://doi.org/10.1016/j.chemosphere.2020.126573, 2020.

Hu, T., Cao, J., Lee, S., Ho, K., Li, X., Liu, S., Chen, J.: Physiochemical characteristics of indoor $PM_{2.5}$ with combustion of dried yak dung as biofuel in Tibetan Plateau, China. Indoor And Built Environment, 25, 737-747, https://doi.org/10.1177/1420326X15586584, 2016.

Huang, K., Fu, J.S., Prikhodko, V.Y., Storey, J.M., Romanov, A., Hodson, E.L., Cresko, J., Morozova, I., Ignatieva, Y., Cabaniss, J.: Russian anthropogenic black carbon: Emission reconstruction and Arctic black carbon simulation. J. Geophys. Res.-Atmos, 120, 11306-11333, https://doi.org/10.1002/2015JD023358, 2015.

Huang, R.J., Yang, L., Shen, J.C., Yuan, W., Gong, Y.Q., Guo, J., Cao, W.J., Duan, J., Ni, H.Y., Zhu, C.S., Dai, W.T., Li, Y.J., Chen, Y., Chen, Q., Wu, Y.F., Zhang, R.J., Dusek, U., O'Dowd, C., Hoffmann, T.: Water-Insoluble Organics Dominate Brown Carbon in Wintertime Urban Aerosol of China: Chemical Characteristics and Optical Properties. Environmental Science & Technology, 54, 7836-7847, https://doi.org/10.1021/acs.est.0c01149, 2020.

https://doi.org/10.5194/egusphere-2026-4493
Preprint. Discussion started: 17 August 2026

Huang, S.: Environmental impacts of polarity-resolved water-soluble organic matter from animal dung burning on the Qinghai-Tibet Plateau [Dataset]. Zenodo, https://doi.org/10.5281/zenodo.21306255, 2026.

Huang, S.S., Luo, Y., Wang, X., Zhang, T., Lei, Y.L., Zeng, Y.L., Sun, J., Che, H.Z., Xu, H.M., Cao, J.J., Shen, Z.X.: Optical properties, chemical functional group, and oxidative activity of different polarity levels of water-soluble organic matter in $PM_{2.5}$ from biomass and coal combustion in rural areas in Northwest China. Atmos. Environ, 283, https://doi.org/10.1016/j.atmosenv.2022.119179, 2022.

Huo, Y., Guo, Z., Li, Q., Wu, D., Chen, J.: Chemical Fingerprinting of HULIS in Particulate Matters Emitted from Residential Coal and Biomass Combustion. Environmental Science & Technology, 55, 3593, https://doi.org/10.1021/acs.est.0c08518, 2021.

Jacobson, M.Z.: Climate response of fossil fuel and biofuel soot, accounting for soot's feedback to snow and sea ice albedo and emissivity. J. Geophys. Res.-Atmos, 109, https://doi.org/10.1029/2004JD004945, 2004.

Janssen, N.A.H., Strak, M., Yang, A., Hellack, B., Kelly, F.J., Kuhlbusch, T.A.J., Harrison, R.M., Brunekreef, B., Cassee, F.R., Steenhof, M., Hoek, G.: Associations between three specific a-cellular measures of the oxidative potential of particulate matter and markers of acute airway and nasal inflammation in healthy volunteers. Occupational And Environmental Medicine, 72, 49-56, https://doi.org/10.1136/oemed-2014-102303, 2015.

Lei, Y.L., Shen, Z.X., Zhang, T., Zhang, Q., Wang, Q.Y., Sun, J., Gong, X.S., Cao, J.J., Xu, H.M., Liu, S.X., Yang, L.: Optical source profiles of brown carbon in size-resolved particulate matter from typical domestic biofuel burning over Guanzhong Plain, China. Sci. Total Environ,622, 244-251, https://doi.org/10.1016/j.scitotenv.2017.11.353, 2018.

Levinson, R., Akbari, H., Berdahl, P.: Measuring solar reflectance-Part I: Defining a metric that accurately predicts solar heat gain. Solar Energy, 84, 1717-1744, https://doi.org/10.1016/j.solener.2010.04.018, 2010.

Lin, M., Yu, J.Z.: Dithiothreitol (DTT) concentration effect and its implications on the applicability of DTT assay to evaluate the oxidative potential of atmospheric aerosol samples. Environ. Pollut, 251, 938-944, https://doi.org/10.1016/j.envpol.2019.05.074, 2019a.

https://doi.org/10.5194/egusphere-2026-4493
Preprint. Discussion started: 17 August 2026

Lin, M., Yu, J.Z.: Effect of metal-organic interactions on the oxidative potential of mixtures of atmospheric humic-like substances and copper/manganese as investigated by the dithiothreitol assay. Sci. Total Environ, 697, 134012, https://doi.org/10.1016/j.scitotenv.2019.134012, 2019b.

Lin, M., Yu, J.Z.: Assessment of Interactions between Transition Metals and Atmospheric Organics: Ascorbic Acid Depletion and Hydroxyl Radical Formation in Organic-Metal Mixtures. Environmental Science and Technology, 54, 1431-1442, https://doi.org/10.1021/acs.est.9b07478, 2020.

Lin, P., Liu, J., Shilling, J.E., Kathmann, S.M., Laskin, J., Laskin, A.: Molecular characterization of brown carbon (BrC) chromophores in secondary organic aerosol generated from photo-oxidation of toluene. Physical Chemistry Chemical Physics, 17, 23312-23325, https://doi.org/10.1039/c5cp02563j, 2015.

Liu H.X, Chen J.Q, Peng, Q.Y, Li, J.L.: Environmental-Health-Low Carbon Benefits and Economic Costs of Household Energy Transition in China. Modern Economic Science, 1-20, https://doi.org/10.20069/j.cnki.DJKX.202401007, 2023.

Mo, Y.Z., Li, J., Jiang, B., Su, T., Geng, X.F., Liu, J.W., Jiang, H.Y., Shen, C.D., Ding, P., Zhong, G.C., Cheng, Z.N., Liao, Y.H., Tian, C.G., Chen, Y.J., Zhang, G.: Sources, compositions, and optical properties of humic-like substances in Beijing during the 2014 APEC summit: Results from dual carbon isotope and Fourier-transform ion cyclotron resonance mass spectrometry analyses. Environ. Pollut, 239, 322-331, https://doi.org/10.1016/j.envpol.2018.04.041, 2018.

Mukherjee, A., Dey, S., Rana, A., Jia, S., Banerjee, S., Sarkar, S.: Sources and atmospheric processing of brown carbon and HULIS in the Indo-Gangetic Plain: Insights from compositional analysis. Environ Pollut, 267, 115440, https://doi.org/10.1016/j.envpol.2020.115440, 2020.

Nakayama, T., Sato, K., Matsumi, Y., Imamura, T., Yamazaki, A., Uchiyama, A.: Wavelength and NOx dependent complex refractive index of SOAs generated from the photooxidation of toluene. Atmos. Chem. Phys, 13, 531-545, https://doi.org/10.5194/acp-13-531-2013, 2013.

Pani, S.K., Lee, C.-T., Griffith, S.M., Lin, N.-H.: Humic-like substances (HULIS) in springtime aerosols at a high-altitude background station in the western North Pacific: Source attribution, abundance, and light-absorption. Sci. Total Environ, 809,

https://doi.org/10.5194/egusphere-2026-4493
Preprint. Discussion started: 17 August 2026

https://doi.org/10.1016/j.scitotenv.2021.151180, 2022.

Peng, H.Y., Wang, Y.S., Wang, Y.L., Chen, Y.K., Li, D., Xue, H.: Characteristics of emission and light-absorption of size-segregated carbonaceous aerosol emitted from four types of coal combustion at different combustion temperatures. Atmos. Pollut. Res, 13, https://doi.org/10.1016/j.apr.2021.101265, 2022.

Qin, J.J., Zhang, L.M., Qin, Y.Y., Shi, S.X., Li, J.N., Gao, Y.W., Tan, J.H., Wang, X.M.: pH-Dependent Chemical Transformations of Humic-Like Substances and Further Cognitions Revealed by Optical Methods. Environmental Science & Technology, 56, 7578-7587, https://doi.org/10.1021/acs.est.1c07729, 2022.

Qiu, Y., Yang, F.A., Lai, W.Y.: The impact of indoor air pollution on health outcomes and cognitive abilities: empirical evidence from China. Population And Environment, 40, 388-410, https://doi.org/10.1007/s11111-019-00317-6, 2019.

Schaap, M., Van Der Gon, H., Dentener, F.J., Visschedijk, A.J.H., Van Loon, M., ten Brink, H.M., Putaud, J.P., Guillaume, B., Liousse, C., Builtjes, P.J.H.: Anthropogenic black carbon and fine aerosol distribution over Europe. J. Geophys. Res.-Atmos, 109, https://doi.org/10.1029/2003JD004330, 2004.

Sun, J., Shen, Z.X., Zhang, B., Zhang, L.M., Zhang, Y., Zhang, Q., Wang, D.W., Huang, Y., Liu, S.X., Cao, J.J.: Chemical source profiles of particulate matter and gases emitted from solid fuels for residential cooking and heating scenarios in Qinghai-Tibetan Plateau. Environ. Pollut, 285, https://doi.org/10.1016/j.envpol.2021.117503, 2021.

Tian, J., Wang, Q.Y., Ma, Y.Y., Wang, J., Han, Y.M., Cao, J.J.: Impacts of biomass burning and photochemical processing on the lightabsorption of brown carbon in the southeastern Tibetan Plateau. Atmos. Chem. Phys, 23, 1879-1892, https://doi.org/ 10.5194/acp-23-1879-2023, 2023.

Tian, T., Ma, J.: Numerical simulation of aerosol direct radiation forcing over the Tibetan Plateau. Climatic and Environmental Research, 26, 449-460, https://doi.org/10.3878/j.issn.1006-9585.2021.20131, 2021.

Voliotis, A., Prokes, R., Lammel, G., Samara, C.: New insights on humic-like substances associated with wintertime urban aerosols from central and southern Europe: Size-resolved chemical characterization and optical properties. Atmos. Environ, 166, 286-299,

https://doi.org/10.5194/egusphere-2026-4493
Preprint. Discussion started: 17 August 2026

https://doi.org/10.1016/j.atmosenv.2017.07.024, 2017.

Wang, D.C., Wang, H.Y., Qu, M., Ma, Y.Y., Wang, K.J., Jia, S.J., Yu, C.J., Zhang, S.P.: Suitability evaluation and potential estimation of photovoltaic power generation and carbon emission reduction in the Qinghai-Tibet Plateau. Environmental Monitoring And Assessment 195. https://doi.org/10.1007/s10661-023-11439-8, 2023.

Wang, J., Zhong, H., Yang, Z., Wang, M., Kammen, D.M., Liu, Z., Ma, Z., Xia, Q., Kang, C.: Exploring the trade-offs between electric heating policy and carbon mitigation in China. Nature Communications, 11, https://doi.org/10.1038/s41467-020-19854-y, 2020.

Wang, Q., Han, Y., Ye, J., Liu, S., Pongpiachan, S., Zhang, N., Han, Y., Tian, J., Wu, C., Long, X., Zhang, Q., Zhang, W., Zhao, Z., Cao, J.: High Contribution of Secondary Brown Carbon to Aerosol Light Absorption in the Southeastern Margin of Tibetan Plateau. Geophysical Research Letters, 46, 4962-4970, https://doi.org/10.1029/2019GL082731, 2019.

Wang, R., Tao, S., Wang, W., Liu, J., Shen, H., Shen, G., Wang, B., Liu, X., Li, W., Huang, Y., Zhang, Y., Lu, Y., Chen, H., Chen, Y., Wang, C., Zhu, D., Wang, X., Li, B., Liu, W., Ma, J.: Black Carbon Emissions in China from 1949 to 2050. Environmental Science & Technology, 46, 7595-7603, https://doi.org/10.1021/es3003684, 2012.

Wang, Y., Zhong, Y., Liao, J., Wang, G.: $PM_{2.5}$-related cell death patterns. International Journal of Medical Sciences, 18, 1024-1029, https://doi.org/10.7150/ijms.46421, 2021.

Win, M.S., Tian, Z., Zhao, H., Xiao, K., Peng, J., Shang, Y., Wu, M., Xiu, G., Lu, S., Yonemochi, S., Wang, Q.: Atmospheric HULIS and its ability to mediate the reactive oxygen species (ROS): A review. J Environ Sci (China), 71, 13-31, https://doi.org/10.1016/j.jes.2017.12.004, 2018.

Wu, G., Cong, Z., Kang, S., K, K., Fu, P., Zhang, Y., Wan, X., Gao, S., Liu, B.: Brown carbon in the cryosphere: current knowledge and perspective. Advances in Climate Change Research, 7, 82-89, https://doi.org/10.1016/j.accre.2016.06.002, 2016.

Wu, J.R., Bei, N.F., Hu, B., Liu, S.X., Zhou, M., Wang, Q.Y., Li, X., Liu, L., Feng, T., Liu, Z.R., Wang, Y.C., Cao, J.J., Tie, X.X., Wang, J., Molina, L.T., Li, G.H.: Aerosol-radiation feedback deteriorates the wintertime haze in the North China Plain. Atmos. Chem. Phys, 19, 8703-8719, https://doi.org/10.5194/acp-19-8703-2019, 2019.

Wu, N., Lu, B., Chen, Q., Chen, J., Li, X.: Connecting the Oxidative Potential of Fractionated

https://doi.org/10.5194/egusphere-2026-4493
Preprint. Discussion started: 17 August 2026

Particulate Matter With Chromophoric Substances. J. Geophys. Res.-Atmos, 127, https://doi.org/10.1029/2021JD035503, 2022.

Xiao, Q., Saikawa, E., Yokelson, R.J., Chen, P., Li, C., Kang, S.: Indoor air pollution from burning yak dung as a household fuel in Tibet. Atmos. Environ, 102, 406-412, https://doi.org/10.1016/j.atmosenv.2014.11.060, 2015.

Xu, X., Lu, X., Li, X., Liu, Y., Wang, X., Chen, H., Chen, J., Yang, X., Fu, T.M., Zhao, Q., Fu, Q.: ROS-generation potential of Humic-like substances (HULIS) in ambient $PM_{2.5}$ in urban Shanghai: Association with HULIS concentration and light absorbance. Chemosphere, 256, 127050, https://doi.org/10.1016/j.chemosphere.2020.127050, 2020.

Yan, C., Ma, S., He, Q., Ding, X., Zheng, M.: Identification of $PM_{2.5}$ sources contributing to both Brown carbon and reactive oxygen species generation in winter in Beijing, China. Atmos. Environ, 246, 118069, https://doi.org/10.1016/j.atmosenv.2020.118069, 2020.

Yao, H., Song, Y., Liu, M., Archer-Nicholls, S., Lowe, D., McFiggans, G., Xu, T., Du, P., Li, J., Wu, Y., Hu, M., Zhao, C., Zhu, T.: Direct radiative effect of carbonaceous aerosols from crop residue burning during the summer harvest season in East China. Atmos. Chem. Phys, 17, 5205-5219, https://doi.org/10.5194/acp-17-5205-2017, 2017.

Yu., H., Wei., J., Cheng., Y., Subedi., K., Verma., V.: Synergistic and Antagonistic Interactions among the Particulate Matter Components in Generating Reactive Oxygen Species Based on the Dithiothreitol Assay. Environmental science & technology, 52, 2261-2270, https://doi.org/10.1021/acs.est.7b04261, 2018.

Zhang, B., Shen, Z.X., Sun, J., He, K., Zou, H.J., Zhang, Q., Li, J.J., Xu, H.M., Liu, S.X., Ho, A., Cao, J.J.: County-level of particle and gases emission inventory for animal dung burning in the Qinghai-Tibetan Plateau, China. Journal Of Cleaner Production, 367, https://doi.org/10.1016/j.jclepro.2022.133051, 2022a.

Zhang, Q., Shen, Z., Zhang, L., Zeng, Y., Cao, J.J.: Investigation of Primary and Secondary Particulate Brown Carbon in Two Chinese Cities of Xi'an and Hong Kong in Wintertime. Environmental Science and Technology, 54, 3803-3813, https://doi.org/10.1021/acs.est.9b05332, 2020.

Zhang, T., Huang, S.S., Wang, D.W., Sun, J., Zhang, Q., Xu, H.M., Ho, S.S.H., Cao, J.J., Shen, Z.X.:

https://doi.org/10.5194/egusphere-2026-4493
Preprint. Discussion started: 17 August 2026

Seasonal and diurnal variation of $PM_{2.5}$ HULIS over Xi'an in Northwest China: Optical properties, chemical functional group, and relationship with reactive oxygen species (ROS). Atmos. Environ, 268, 118782, https://doi.org/10.1016/j.atmosenv.2021.118782, 2022b.

Zhang, T., Shen, Z.X., Huang, S.S., Lei, Y.L., Zeng, Y.L., Sun, J., Zhang, Q., Ho, S.S.H., Xu, H.M., Cao, J.J.: Optical properties, molecular characterizations, and oxidative potentials of different polarity levels of water-soluble organic matters in winter $PM_{2.5}$ in six China's megacities. Sci. Total Environ, 853, https://doi.org/10.1016/j.scitotenv.2022.158600, 2022c.

Zhang, T., Shen, Z.X., Zeng, Y.L., Cheng, C.L., Wang, D.W., Zhang, Q., Lei, Y.L., Zhang, Y., Sun, J., Xu, H.M., Ho, S.S.H., Cao, J.J.: Light absorption properties and molecular profiles of HULIS in $PM_{2.5}$ emitted from biomass burning in traditional "Heated Kang" in Northwest China. Sci. Total Environ, 776, 146014, https://doi.org/10.1016/j.scitotenv.2021.146014, 2021.

Zhang, X.L., Chen, X., Wang, J.: A number-based inventory of size-resolved black carbon particle emissions by global civil aviation. Nature Communications,10, https://doi.org/10.1038/s41467-019-08491-9, 2019.

Zhou, R., Chen, Q., Chen, J., Ren, L., Mochida, M.: Distinctive Sources Govern Organic Aerosol Fractions with Different Degrees of Oxygenation in the Urban Atmosphere. Environmental Science and Technology, 55, 4494-4503, https://doi.org/10.1021/acs.est.0c08604, 2021.